Available online at www.sciencedirect.com
SCIENCE DIRECT
Journal of Physics and Chemistry of Solids 66 (2005) 839–844
JOURNAL OF PHYSICS AND CHEMISTRY OF SOLIDS
www.elsevier.com/locate/jpcs

Electron hopping mechanism in hematite (α-Fe_2O_3)

John C. Papaioannou[a,*], George S. Patermarakis[b], Haido S. Karayianni[b]

[a]*Laboratory of Physical Chemistry, Department of Chemistry, University of Athens, 15771 Athens, Greece*
[b]*Laboratory of Physical Chemistry, Department of Materials Science and Engineering, School of Chemical Engineering, National Technical University of Athens, Iroon Polytechniou 9, Zografou, 157 80 Athens, Greece*

Received 29 March 2004; revised 16 November 2004; accepted 23 November 2004

Abstract

The frequency dependence of the real (ε') and imaginary (ε'') parts of the dielectric constant of polycrystalline hematite (α-Fe_2O_3) has been investigated in the frequency range 0–100 kHz and the temperature range 190–350 K, in order to reveal experimentally the electron hopping mechanism that takes place during the Morin transition of spin-flip process. The dielectric behaviour is described well by the Debye-type relaxation (α-dispersion) in the temperature regions $T<233$ K and $T>338$ K. In the intermediate temperature range 233 K $<T<338$ K a charge carrier mechanism takes place (electron jump from the O^{2-} ion into one of the magnetic ions Fe^{3+}) which gives rise to the low frequency conductivity and to the Ω-dispersion. The temperature dependence of relaxation time (τ) in the $-\ln\tau$ vs $10^3/T$ plot shows two linear regions. In the first, $T<238$ K, τ increases with increasing T implying a negative activation energy -0.01 eV, and in the second region $T>318$ K τ decreases as the temperature increases implying a positive activation energy 0.12 eV. The total reorganization energy (0.12–0.01) 0.11 eV is in agreement with the adiabatic activation energy 0.11 eV given by an ab initio model in the literature. The temperature dependence of the phase shift in the frequencies 1, 5, 10 kHz applied shows clearly an average Morin temperature $T_{Mo}=284\pm1$ K that is higher than the value of 263 K corresponding to a single crystal due to the size and shape of material grains.

Keywords: A. Magnetic materials; D. Dielectric properties

1. Introduction

The crystal structure of α-Fe_2O_3 (hematite) is that of corundum α-Al_2O_3, i.e. an approximately hexagonal closed-packed array of oxygen ions O^{2-} with Fe^{3+} ions occupying two-thirds of the available octahedral sites [1].

The magnetic structure of α-Fe_2O_3, studied by neutron diffraction [2,3], showed an antiferromagnetic material (Néel temperature $T_N=960$ K). Below the Néel temperature the bulk material presents a spin-flip magnetic transition at $T_{Mo}=263$ K, the so-called Morin transition [4]. Mössbauer spectroscopy [5] confirmed that below T_{Mo} the magnetically ordered spins are oriented along the trigonal [111] axis (c-axis) and the material behaves as a perfect antiferromagnetic one (AF). Above T_{Mo} the spins lie in the basal plane perpendicular to the [111] axis, except for a slight spin canting ($\sim$1 min of the arc) out of the basal plane which is responsible for the imperfect antiferromagnetic coupling of the Fe^{3+} ions in the alternating sublattices and finally for the net weak-ferromagnetic (WF) moment. The magnetic axis of each iron atom flips instantaneously from 0 to 90° as the temperature increases above T_{Mo}.

The Morin transition arises from the coexistence of two competitive anisotropy components of the total energy with comparable magnitudes, opposite signs and different temperature dependences: (i) The long-range *magnetic dipolar* anisotropy component energy ($K_{MD}<0$) which is negative and falls off only as the inverse cube of the dipole separation distance. (ii) The local *fine structure* anisotropy component ($K_{FS}>0$) which is positive arising from the higher order of spin-orbit coupling of the individual metal ions and is quite short-ranged falling off exponentially with the spin separation distance [6]. The two components have different temperature dependences. The total anisotropy energy at $T<T_{Mo}$ is positive because $|K_{FS}|>|K_{MD}|$ and at

* Corresponding author.
E-mail address: jpapaio@cc.uoa.gr (J.C. Papaioannou).

0022-3697/$ - see front matter © 2004 Elsevier Ltd. All rights reserved.
doi:10.1016/j.jpcs.2004.11.002

$T > T_{Mo}$ it becomes negative because $|K_{FS}| < |K_{MD}|$. The change in total energy sign at T_{Mo} is responsible for the spin-flip transition.

The main contribution to the magnetic dipolar interaction energy K_{MD} arises from the superexchange mechanism [7] that takes place between the two magnetic Fe^{3+} ions through the intermediary nonmagnetic O^{2-} ions and is most effective when the Fe_a^{3+}–O^{2-}–Fe_b^{3+} bond angle approaches 180°. In order to explain the superexchange mechanism, Kramers [8] postulated that there is a finite probability for an electron to jump from an p-state of O^{2-} ion to an s-state of one of the magnetic ions (e.g. Fe_a^{3+}) and the p-electron remaining in the negative ion O^- interacts strongly with the other magnetic ion Fe_b^{3+}. According to a recent ab initio model for hematite, an electron is transferred from one iron atom to another by a II/III valence alternation (hopping mechanism) [9].

Earlier it has been shown that the temperature dependence of dielectric properties can reveal order–disorder transitions or hydrogen bond transformations (flip-flop to normal type) indicated by a peak in the imaginary part of dielectric constant ε'' and by a minimum in the phase shift φ of the current passing through the sample relative to the applied voltage component [10]. When the sample presents ionic or electronic conductivity the φ vs. T plots clearly reveal the transition at any applied frequency while the peak in the ε'' vs. T plots is suppressed as frequency increases.

In the present work the dielectric parameters (ε', ε'', φ) of polycrystalline hematite over the frequency range 0–100 kHz and temperature range 190–350 K are investigated in order to reveal experimentally the electron hopping mechanism occurring during the Morin transition of spin-flip process.

2. Experimental

Samples of freshly prepared high purity (>99.95%) polycrystalline α-Fe_2O_3 [11], made of pressed powder cylindrical pellets 10 mm in diameter and thickness 1.6 mm by a Riken Powder Press model P-1B instrument, were prepared. Two platinum foil electrodes 10 mm in diameter were adjusted on both sides of samples and pressed simultaneously with them. Each sample was loaded to the temperature control chamber between two brass rods accompanied by a compression spring. The sample was combined in series with a constant known resistance R_i, in which the applied signal V yielded a voltage drop V_i. V_i was <0.1 V so that its effect on the phase shift was minimized. The dielectric measurements were taken using a low frequency (0–100 kHz) Dynamic Signal Analyser (DSA, Hewlett–Packard 3561A), over the temperature range 190–350 K, which was connected to a PC for further processing of data stored in the analyser. The analytical experimental procedure was described in details elsewhere [10].

3. Results

3.1. The frequency dependence of dielectric constant

The frequency (f) dependence of the real (ε') and imaginary (ε'') parts of the dielectric constant in the frequency range 0–100 kHz are shown in Figs. 1–3 for the temperature ranges A (195–249 K), B (256–313 K) and C (318–348 K), respectively.

In the (A) temperature range, Fig. 1, the ε' vs. frequency curves have generally a sigmoid profile with an inflection point at about 40 kHz. These curves become parallel to

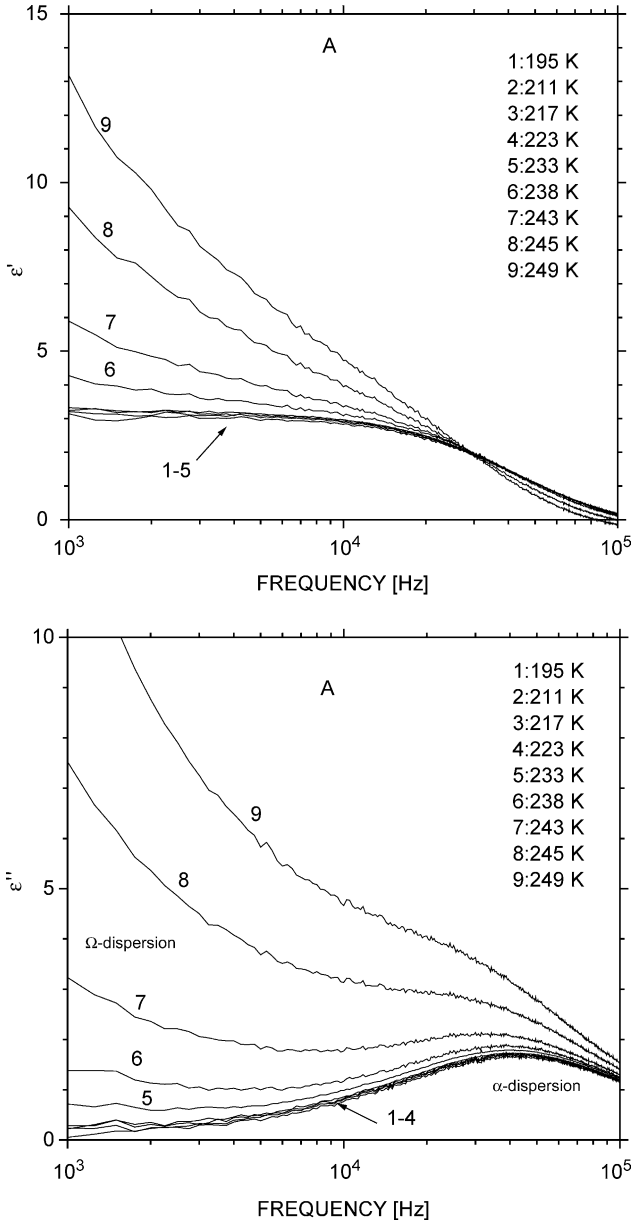

Fig. 1. Frequency dependence of the real (ε') and imaginary (ε'') parts of the dielectric constant of α-Fe_2O_3 for constant temperatures in the temperature range (A) 1, 195 K; 2, 211 K; 3, 217 K; 4, 223 K; 5, 233 K; 6, 238 K; 7, 243 K; 8, 245 K; and 9, 249 K.

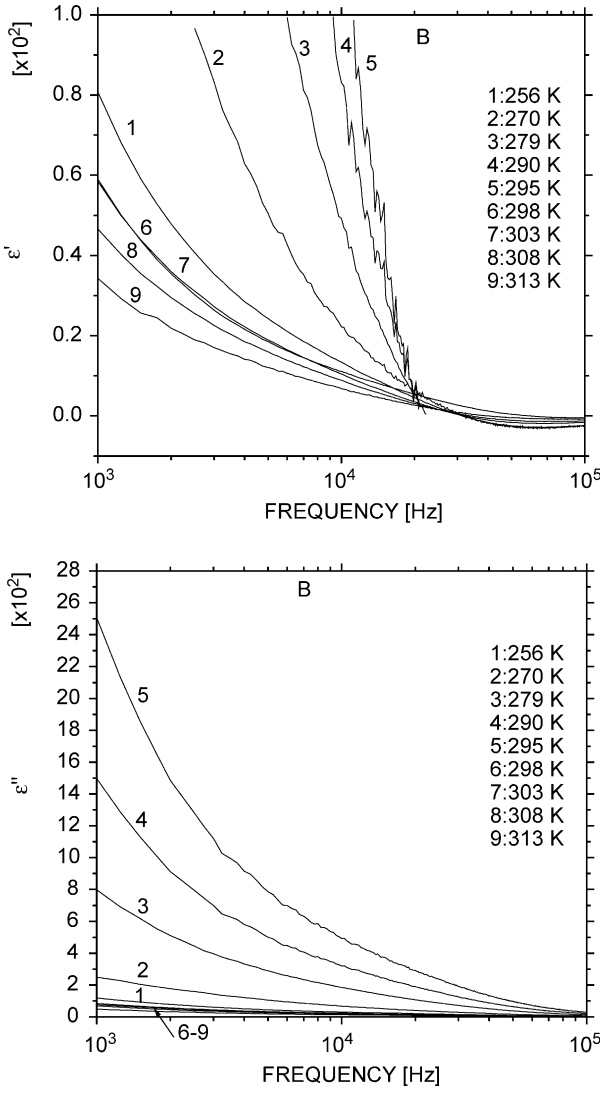

Fig. 2. Frequency dependence of the real (ε') and imaginary (ε'') parts of the dielectric constant of α-Fe_2O_3 for constant temperatures in the temperature range (B) 1, 256 K; 2, 270 K; 3, 279 K; 4, 290 K; 5, 295 K; 6, 298 K; 7, 303 K; 8, 308 K and 9, 313 K.

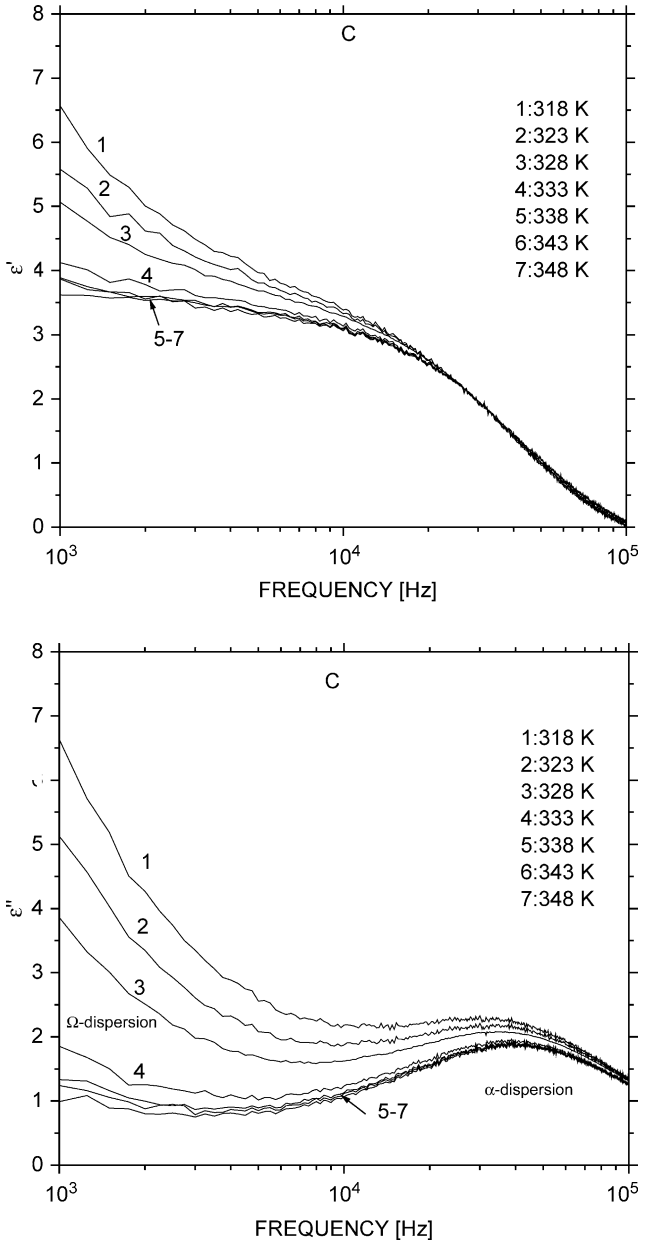

Fig. 3. Frequency dependence of the real (ε') and imaginary (ε'') parts of the dielectric constant of α-Fe_2O_3 for constant temperatures in the temperature range (C) 1, 318 K; 2, 323 K; 3, 328 K; 4, 333 K; 5, 338 K; 6, 343 K and 7, 348 K.

the horizontal axis at temperatures close to 195 K, where $\varepsilon' = 3.1$. In the other temperatures the corresponding slopes of the ε' vs. frequency plots increase with increasing temperature. The frequency variation of ε'' at 195 K has the form of a bell-like curve (α-dispersion) centred at a characteristic frequency $f_{max} = 43{,}135$ Hz with $\varepsilon''_{max} = 1.7$ and a half-height width 0.9 decades of frequency. Similar curves are observed for temperatures 211, 217, 223 K. A rapid rise of ε'' is observed by decreasing frequency (Ω-dispersion) in the range $f < 10^4$ kHz for temperatures 233, 238, 243, 245 K (curves 5–8) while the corresponding value of ε''_{max} increases with temperature. For 249 K the Ω-dispersion (curve 9) is completely superimposed over the α-dispersion and the ε''_{max} cannot be distinguished.

In the (B) temperature range, Fig. 2, both ε', ε'' vs. frequency plots show that the ε' and ε'' values decrease with frequency at each constant temperature. The corresponding ε', and ε'' values at a specific frequency 1 kHz increase with temperature up to their maximum values (curves 1–5) and then decrease as the temperature increases (curves 6–9) up to the values $\varepsilon' = 34.2$ and $\varepsilon'' = 48.6$ at 313 K. This temperature region is characterized by the presence of a strong Ω-dispersion and the absence of α-dispersion.

In the (C) temperature range, Fig. 3, the ε', and ε'' vs. frequency plot profiles are similar to those of the (A) temperature range and both Ω- and α-dispersions appear, but their temperature dependence is the reverse one. For example at frequency 1 kHz the values decrease from $\varepsilon' = 6.6$ and $\varepsilon'' = 6.5$ at 318 K (curve 1) to $\varepsilon' = 3.6$ and $\varepsilon'' = 1.0$ at

348 K curve 7). Similarly the ε''_{max} values (α-dispersion) decrease from 2.3 to 1.9. The Ω-dispersion is also reduced as the temperature increases and finally at the temperature of 348 K (curve 7) it completely disappears and only the α-dispersion still remains.

3.2. The temperature dependence of the phase shift and the relaxation time

The phase shift (φ) of α-Fe_2O_3 at a fixed frequency 1 kHz (Fig. 4) in the range 190–350 K, drops from 89° at 195 K to

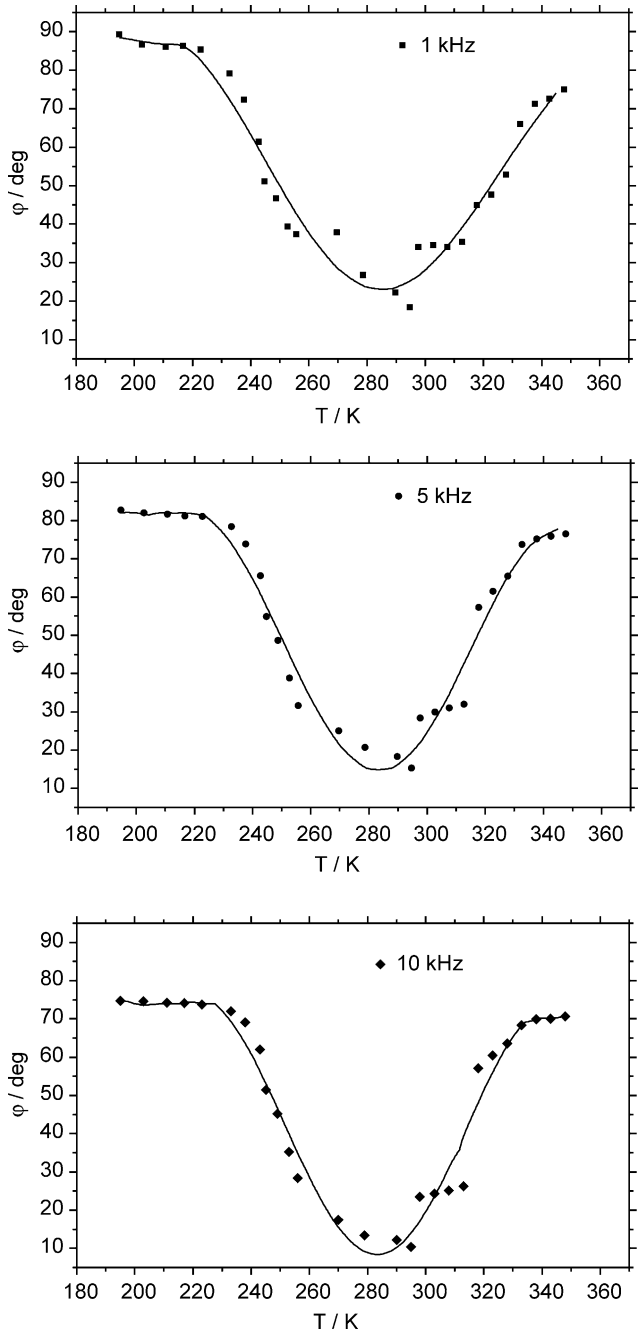

Fig. 4. Temperature dependence of phase shift, φ, for a-Fe_2O_3, at frequencies 1 kHz, 5 kHz and 10 kHz.

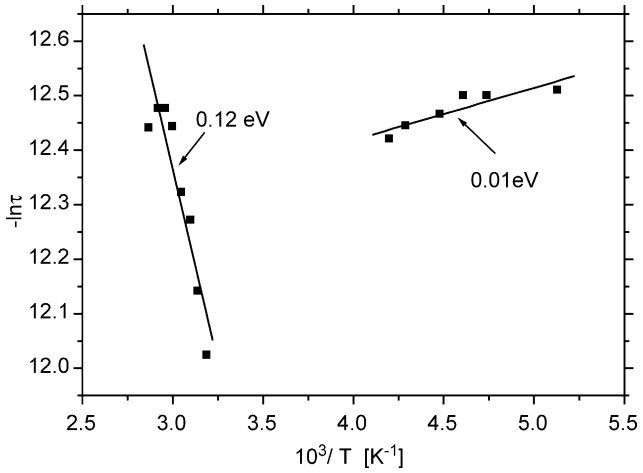

Fig. 5. Plot of $-\ln\tau$ vs. $10^3/T$ for α-Fe_2O_3.

a minimum 22.9° at 285.5 K and then increases up to 76.8° at 348 K. Similarly, the plots of the phase shift vs. T for the 5, and 10 kHz applied behave in the same way revealing minimum values 14.5° at 282.4 K and 8.39° at 283.1 K, respectively.

The temperature dependence of relaxation time ($\tau = 1/2\pi f_{max}$), where f_{max} is the frequency that corresponds to the ε''_{max}, shows two linear regions in the $-\ln\tau$ vs. $10^3/T$ plot of Fig. 5 in one of which, $T<238$ K, τ increases and in the other $T>318$ K τ decreases with temperature.

4. Discussion

The dependence of ε' and ε'' on frequency in the temperature ranges (A) and (C), Figs. 1 and 3, is well described by the Debye [12] relaxation according to the following equations:

$$\varepsilon' = \varepsilon_\infty + (\varepsilon_s - \varepsilon_\infty)/(1+\omega^2\tau^2) \quad (1)$$

$$\varepsilon'' = (\varepsilon_s - \varepsilon_\infty)\omega\tau/(1+\omega^2\tau^2) + \sigma/\omega\varepsilon_0 \quad (2)$$

$$\varepsilon''_{max} = (\varepsilon_s - \varepsilon_\infty)/2, \quad (3)$$

where ε_s is the static dielectric constant, ε_∞ is the dielectric constant at very high frequencies, ε_0 is the vacuum dielectric permittivity, σ is the dc conductivity of the system, τ is the single Debye relaxation time and ω is the angular frequency of the applied field. Eq. (1) describes a sigmoid ε' vs. frequency plot, with horizontal values $\varepsilon_s - \varepsilon_\infty$ and ε_∞. In Figs. 1 and 3 perfect sigmoid plots are observed for $T<233$ K and $T>338$ K, respectively. In the other temperatures the plots profiles deviate from a sigmoid one. Eq. (2) for $\sigma=0$ presents a peak (α-dispersion) in the ε'' vs. frequency plot and the $\varepsilon''_{max} = (\varepsilon_s - \varepsilon_\infty)/2$ value is independent of temperature. Eq. (2) for $\sigma \neq 0$ presents a peak (α-dispersion) with a rapid rise of ε'' at low frequencies (Ω-dispersion), which is proportional to σ and inversely

proportional to the frequency ω as it was shown in Figs. 1 and 3. Fig. 1 shows that on increasing temperature the induced polarization (ε', and ε'') increases resulting in a charge delocalization that destabilizes the antiferromagnetic state. This charge corresponds at least to one p-electron that is released from the oxygen ion O^{2-} in order to be trapped from a neighbouring iron ion Fe^{3+} according to Kramers model [8]. The large ε', ε'' values around the Morin transition temperature of Fig. 2 are caused to the dc conductivity σ according to (2) that is analogous to the charge transferred from site to site. Fig. 3 shows that on increasing temperature the induced polarization (ε' and ε'') decreases resulting in a charge localization that stabilizes the ferromagnetic state. During this stage the released electron is bound to the iron ion Fe^{3+}. The same procedure is repeated between neighbouring Fe and O atoms implying the establishment of an electron hopping mechanism. To this result advocates the ab initio model given earlier [9] according to which the electron carrying charge behaves as a localized particle and is transferred from one iron atom to another yielding successively Fe^{2+} instead of Fe^{3+} in the lattice. This mechanism is consistent with the temperature dependence of relaxation time shown in Fig. 5 in which $-\ln \tau$ varies linearly with $10^3/T$. The phenomenon of the increase of relaxation time τ with increasing temperature implies a negative activation energy, which suggests that the activation process involves the detachment of the electron from the O^{2-} ion. The decrease of relaxation time τ with T implies a positive activation energy suggesting the bound of the electron to the Fe^{3+} ion and the formation of an Fe^{2+} ion. The activation energies E calculated by the application of the Arrhenius equation

$$\tau = \tau_0 \exp(-E/RT) \text{ or } \ln \tau = \ln \tau_0 - E/RT \quad (4)$$

in the linear regions of the $-\ln \tau$ vs. $10^3/T$ plot, Fig. 5, are -0.01 eV for $T<238$ K (as the T increases τ increases implying negative activation energy) and $+0.12$ eV for $T>318$ K (as the T increases τ decreases implying positive activation energy). The total reorganization energy is (0.12–0.01) 0.11 eV is in agreement with the adiabatic activation energy $\Delta G^* = 0.11$ eV required to allow the electron hopping from one site to a next, predicted by the ab initio model recently published [9].

The temperature dependence of phase shift in the frequencies 1, 5 and 10 kHz applied, Fig. 5, shows clearly an average Morin temperature $T_{Mo} = 284 \pm 1$ K that is higher than the previously mentioned 263 K value corresponding to a single crystal hematite. The Morin transition temperature (T_{Mo}) is influenced by the method of preparing the sample, the size and the shape of grains of material [13], etc. From Fig. 5 it is inferred that the AF state is stable at $T<$ 220 K and the WF state at $T>320$ K. In the intermediate region $220\text{ K} < T < 320\text{ K}$ coexist both anisotropy components $|K_{FS}|$, $|K_{MD}|$ and at $T = T_{Mo}$ $|K_{FS}| = |K_{MD}|$.

5. Conclusions

The dielectric behaviour of α-Fe_2O_3 is described well by the Debye-type relaxation (α-dispersion) in the temperature regions $T<233$ K and $T>338$ K. In the intermediate temperature region $233\text{ K} < T < 338\text{ K}$ an electron hopping mechanism takes place (electron jump from the O^{2-} ion to one of the neighbouring Fe^{3+} ions which gives rise to the dc-conductivity (ac-conductivity at low frequencies) and the Ω-dispersion.

The relaxation time varies exponentially with temperature showing two linear regions in the $-\ln \tau$ vs. $10^3/T$ plots characterized by activation energies -0.01 eV for $T<238$ K and $+0.12$ eV for $T>318$ K. The first is ascribed to the energy of detachment of an electron from the O^{2-} ion and the second to the energy of capture of an electron from an Fe^{3+} ion yielding Fe^{2+}. The total reorganization energy (0.12–0.01) 0.11 eV is consistent with the adiabatic activation energy $\Delta G^* = 0.11$ eV predicted by the ab initio model recently published [9].

The temperature dependence of the phase shift in the frequencies 1, 5 and 10 kHz applied shows clearly an average Morin temperature $T_{Mo} = 284 \pm 1$ K that is higher than the value of 263 K corresponding to a single crystal hematite due to the size and shape of material grains.

Acknowledgements

The authors are pleased to acknowledge Dr Anthoula Dimirkou member of Soil Science Institute of Athens for offering the samples of hematite.

References

[1] M. Fuller, Experimental methods in rock magnetism and paleomagnetism in: C.G. Sammis, T.L. Henyey (Eds.), Methods of Experimental Physics vol. 24A, Academic Press, Orlando, 1987, pp. 303–471; L. Pauling, S.B. Hendricks, The crystal structure of hematite and corundum, J. Am. Chem. Soc. 47 (1925) 781–790.
[2] C.G. Shull, J.S. Smart, Detection of antiferromagnetism by neutron diffraction, Phys. Rev. 76 (1949) 1256–1257.
[3] C.G. Shull, W.A. Strauser, O.E. Wollan, Neutron diffraction by paramagnetic and antiferromagnetic substances, Phys. Rev. 83 (1951) 333–345.
[4] F.J. Morin, Magnetic susceptibility of α-Fe_2O_3 and α-Fe_2O_3 with added titanium, Phys. Rev. 78 (1950) 819–820; F.J. Morin, Electrical properties of α-Fe_2O_3 and α-Fe_2O_3 containing titanium, Phys. Rev. 83 (1951) 1005–1010.
[5] N.N. Greenwood, C.T. Gibb, Mössbauer spectroscopy, Chapman and Hall, London, 1971. p. 240.
[6] J.O. Artman, J.C. Murphy, S. Foner, Magnetic anisotropy in antiferromagnetic corundum-type sesquioxides, Phys. Rev. 138 (1965) A912–A917.
[7] P.W. Anderson, Antiferromagnetism. Theory of superexchange interaction, Phys. Rev. 79 (1950) 350–356.

[8] H.A. Kramers, Physica 1 (1934) 182.
[9] K.M. Rosso, D.M.A. Smith, M. Dupuis, An ab initio model of electron transport in hematite (α-Fe_2O_3) basal planes, J. Chem. Phys. 118 (2003) 6455–6466.
[10] J.C. Papaioannou, N.D. Papadimitropoulos, I.M. Mavridis, Dielectric relaxation of β-cyclodextrin complex with 4-*t*-butylbenzyl alcohol, Mol. Phys. 97 (1999) 611–627.
[11] A. Dimirkou, A. Ioannou, Ch. Kallianou, Synthesis-identification of hematite and kaolinite–hematite (k–h) system, Commun. Soil Sci. Plan Anal. 27 (1996) 1091–1106.
[12] C.P. Smyth, Dielectric behaviour and structure, McGraw-Hill, New York, 1955. pp. 52–62, Chapter 2.
[13] G.J. Muench, S. Arajs, E. Matijevic, The Morin transition in small alpha-Fe2O3 particles, Phys. Status Solidi A 92 (1985) 187–192.